

**SYNTHESIS AND CHARACTERIZATION
OF THERMORESPONSIVE
POLY(*N*-ISOPROPYLACRYLAMIDE)-DNA
BIOCONJUGATES**

OOI WEI YANG

UNIVERSITI SAINS MALAYSIA

2012

**SYNTHESIS AND CHARACTERIZATION OF THERMORESPONSIVE
POLY(*N*-ISOPROPYLACRYLAMIDE)-DNA BIOCONJUGATES**

by

OOI WEI YANG

**Thesis submitted in fulfillment of the requirements
for the degree of
Doctor of Philosophy**

July 2012

ACKNOWLEDGEMENTS

I wish to thank God and everyone that has made this thesis possible.

Supervisors,

Professor Dr. K. Sudesh Kumar – for the opportunity and guidance.

Professor Dr. Maeda Mizuo – for the hospitality and sharing of wisdom.

Dr. Fujita Masahiro – for the mentoring and guidance.

Friends and colleagues,

Ecobiomaterial lab members – for your friendship and assistance.

Bioengineering lab members and friends in RIKEN especially Dr. Pan Pengju– for your friendship, teamwork/collaborations and constructive brainstorming/sharing of opinions.

Universiti Sains Malaysia – for the Fellowship and candidature matters.

RIKEN – for the scholarship and opportunity to carry out this work as International Program Associate.

Last but not least,

Mom, Dad, Li Ching and family – for the love, encouragement and support.

TABLE OF CONTENTS

ACKNOWLEDGEMENTS.....	ii
TABLE OF CONTENTS.....	iii
LIST OF TABLES.....	vi
LIST OF FIGURES.....	vii
LIST OF ABBREVIATIONS.....	x
LIST OF SYMBOLS.....	xii
ABSTRAK.....	xv
ABSTRACT.....	xviii
CHAPTER ONE Introduction.....	1
1.1 General Introduction.....	1
1.2 Hypothesis and Aims of Thesis.....	6
CHAPTER TWO Literature Review.....	9
2.1 Bioconjugates.....	9
2.1.1 Peptide/protein Bioconjugates.....	12
2.1.2 Carbohydrate Bioconjugates.....	15
2.1.3 Nucleotides/DNA Bioconjugates.....	16
2.1.3.1 DNA Bioconjugates as Gene Delievery Systems.....	17
2.1.3.2 DNA Bioconjugates in Nanoscience.....	18
2.1.3.3 DNA–PNIPAAm Bioconjugates.....	23
2.2 “Smart” Polymeric Materials.....	27
2.2.1 Thermo-Responsive Polymers.....	28
2.2.2 PNIPAAm.....	30
2.2.3 PNIPAAm Copolymers.....	32
2.3 Bioconjugates Synthesis Strategies.....	35
2.3.1 Coupling/ligation Bioconjugation.....	37
2.3.1.1 “Click Chemistry”.....	39
2.3.2 Macroinitiators Bioconjugation.....	41
2.3.3 Inverse Bioconjugation.....	43
2.3.4 Macromonomers Bioconjugation.....	46
CHAPTER THREE Synthesis of PNIPAAm–graft–DNA Bioconjugates via	
Radical Copolymerization.....	47
3.1 Introduction and Experimental Approach.....	47
3.2 Materials and Methods.....	48
3.2.1 Materials.....	48
3.2.2 Synthesis of Vinyl-Derivatized DNA Macromonomer.....	48

3.2.3	Synthesis of PNIPAAm Grafted with ssDNA (PNIPAAm- <i>graft</i> -DNA)	49
3.2.4	Gel Permeation Chromatography (GPC) Measurements.....	52
3.2.5	Differential Scanning Calorimetry (DSC) Measurements.....	52
3.3	Results and Discussion.....	53
3.3.1	Synthesis of PNIPAAm- <i>graft</i> -DNA.....	53
CHAPTER FOUR Structural Characterization of PNIPAAm-<i>graft</i>-DNA		
	<i>Bioconjugate Colloidal Nanoparticles</i>	57
4.1	Introduction and Experimental Approach.....	57
4.2	Materials and Methods.....	58
4.2.1	Dynamic Light Scattering (DLS) Measurements.....	58
4.2.2	Small-Angle X-ray Scattering (SAXS) Methodology.....	59
4.3	Results and Discussion.....	67
4.3.1	Phase Transition of PNIPAAm- <i>graft</i> -DNA.....	67
4.3.2	SAXS Analysis of PNIPAAm- <i>graft</i> -DNA Colloidal Nanoparticle....	75
CHAPTER FIVE Non-Crosslinking Aggregation Analysis of		
	<i>PNIPAAm-<i>graft</i>-DNA particles</i>	80
5.1	Introduction and Experimental Approach.....	80
5.2	Materials and Methods.....	82
5.2.1	UV-Vis Spectroscopy.....	82
5.2.2	SAXS Analysis.....	82
5.3	Results and Discussion.....	86
5.3.1	Decrease Colloidal Stability in PNIPAAm- <i>graft</i> -DNA Particles Induced by cDNA Hybridization.....	86
5.3.2	SAXS Analysis of the Non-Crosslinking Aggregation of PNIPAAm- <i>graft</i> -DNA Particles.....	88
CHAPTER SIX Novel Route for Controlled Synthesis of PNIPAAm-<i>block</i>-DNA		
	<i>Bioconjugates via ATRP and “Click Chemistry”</i>	94
6.1	Introduction and Experimental Approach.....	94
6.2	Materials and Methods.....	96
6.2.1	Materials.....	96
6.2.2	Synthesis of 5'-Alkyne Modified Oligonucleotide.....	98
6.2.3	ATRP of PNIPAAm Homopolymers.....	101
6.2.4	Preparation of PNIPAAm- <i>block</i> -DNA Bioconjugates via “Click Chemistry”	102
6.2.5	Nuclear Magnetic Resonance (NMR) Spectroscopy.....	105
6.2.6	MALDI-TOF Analysis.....	105
6.2.7	GPC Measurements.....	105
6.2.8	DSC Measurements.....	106

6.2.9	UV-Vis Spectroscopy.....	106
6.3	Results and Discussion.....	107
6.3.1	PNIPAAm Homopolymers.....	107
6.3.2	Synthesis and Phase Transition of PNIPAAm- <i>block</i> -DNA Bioconjugates.....	112
CHAPTER SEVEN Characterization of Linear and Four-Miktoarm Star-Shaped PNIPAAm-<i>block</i>-DNA Bioconjugates.....		119
7.1	Introduction and Experimental Approach.....	119
7.2	Materials and Methods.....	121
7.2.1	DLS Measurements.....	121
7.2.2	SAXS Methodology.....	122
7.2.3	Encapsulation and Release of Nile Red Verified by Fluorescence Spectroscopy.....	122
7.3	Results and Discussion.....	123
7.3.1	Thermo-triggered Micellation of PNIPAAm- <i>block</i> -DNA Bioconjugates.....	123
7.3.2	Thermoresponsive Encapsulation and Release of Nile Red by PNIPAAm- <i>block</i> -DNA Bioconjugates.....	126
7.3.3	Internal Structure of PNIPAAm- <i>block</i> -DNA Bioconjugates Colloidal Nanoparticles.....	128
CHAPTER EIGHT Conclusion.....		138
REFERENCES.....		142
APPENDIX A Supplemental methods.....		163
APPENDIX B Structural Model Programming codes.....		169
List of Publications and Conferences.....		176

LIST OF TABLES

	Page
Table 2.1 Examples of peptide/protein bioconjugate and its unique properties.	15
Table 2.2 Examples of “smart” polymeric materials.	28
Table 2.3 Examples of thermo-responsive polymers with LCST or UCST behavior.	29
Table 3.1 Molecular characteristics of PNIPAAm- <i>graft</i> -DNA.	53
Table 4.1 Hydrodynamic radii (R_h), radii of gyration (R_g) and particle association number (N_{ass}) of PNIPAAm- <i>graft</i> -DNA colloidal nanoparticle.	70
Table 4.2 Structural parameters for PNIPAAm- <i>graft</i> -DNA colloidal nanoparticles.	78
Table 5.1 Structural parameters for non-crosslinking aggregation of PNIPAAm- <i>graft</i> -DNA particles.	90
Table 6.1 Target degree of polymerization (DP), yield and molecular weights of linear and three-arm star PNIPAAm homopolymers.	108
Table 6.2 Molecular weights and compositions of linear and four-miktoarm star PNIPAAm- <i>block</i> -DNA bioconjugates.	115
Table 7.1 Hydrodynamic radii (R_h) and gyration of radii (R_g) and particle association number (N_{ass}) of PNIPAAm- <i>block</i> -DNA colloidal nanoparticles.	130
Table 7.2 Structural parameters of PNIPAAm- <i>block</i> -DNA colloidal nanoparticles.	137
Table 8.1 Comparison of PNIPAAm- <i>block</i> -DNA synthesized via novel route of ATRP and “click chemistry” and PNIPAAm- <i>graft</i> -DNA synthesized via conventional radical copolymerization.	141

LIST OF FIGURES

	Page
Figure 1.1 Self assembly of PNIPAAm- <i>graft</i> -DNA bioconjugates into colloidal nanoparticles and the colloidal stability dependence on its DNA structure.	5
Figure 1.2 Outline and flow of thesis.	8
Figure 2.1 A comparison of biological versus synthetic systems with respect to complexity and diversity.	11
Figure 2.2 Artificial oxygen carrier constructed by conjugating hemoglobin molecules to biodegradable polymeric micelles.	14
Figure 2.3 Morphologies transformation of ssDNA- <i>block</i> -PPO micelles upon hybridization with different length of DNA templates to form dsDNA.	22
Figure 2.4. Colloidal stability dependence of PNIPAAm-DNA micelles.	25
Figure 2.5. Turbidimetric ATP detection system by PNIPAAm-DNA bioconjugates.	26
Figure 2.6. Chemical structure and phase transition of PNIPAAm.	31
Figure 2.7 Examples of PNIPAAm copolymer architectures.	34
Figure 2.8 Schematic illustration of the established bioconjugation strategies.	36
Figure 2.9 Coupling reactions for the synthesis of DNA bioconjugates.	38
Figure 2.10 An inverse bioconjugation strategy for oligonucleotide polymer bioconjugates.	45
Figure 3.1 Schematic of PNIPAAm- <i>graft</i> -DNA bioconjugate synthesis.	51
Figure 3.2 A. DSC thermograms of PNIPAAm- <i>graft</i> -DNA copolymers and B. the endothermic peak temperature (T_p) values of ss-0.26 copolymer plotted against NaNO_3 concentration.	56
Figure 4.1 Schematic of synchrotron radiation solution SAXS experiments carried out at SPring-8 Harima, Japan.	62
Figure 4.2 Schematic radial density profile of core-shell structural model.	66
Figure 4.3 Hydrodynamic radii (R_h) distributions and polydispersity indexes (μ_2/Γ^2) of colloidal nanoparticles formed from PNIPAAm- <i>graft</i> -DNA bioconjugates.	71

	Page
Figure 4.4	SAXS intensities of ss-0.26 bioconjugate taken at elevated temperatures. 72
Figure 4.5	Kratky plots of ss-0.26 bioconjugate at elevated temperatures. 73
Figure 4.6	The radii of gyration (R_g) (filled symbols) and particle association number of copolymer chains per particle (N_{ass}) (open symbols) plotted against temperature for PNIPAAm- <i>graft</i> -DNA bioconjugates. 74
Figure 4.7	SAXS analysis of the nanostructures of PNIPAAm- <i>graft</i> -DNA colloidal nanoparticles by employing core-shell model fitting. 79
Figure 5.1	Baxter sticky hard-sphere model. 85
Figure 5.2	Decrease colloidal stability in PNIPAAm- <i>graft</i> -DNA particles induced by cDNA hybridization. 87
Figure 5.3	SAXS profiles (symbol) from PNIPAAm- <i>graft</i> -DNA bioconjugates particles aggregates and their theoretical fitting curves (line). 90
Figure 5.4	Hydrodynamic radii (R_h) dependence of NaNO ₃ concentration of PNIPAAm- <i>graft</i> -DNA bioconjugates. 91
Figure 6.1	Synthetic route of linear diblock and four-miktoarm star PNIPAAm- <i>block</i> -DNA bioconjugates. 99
Figure 6.2	Reverse-phase high-performance liquid chromatography (RP-HPLC) chromatograms of 5'-amino and 5'-alkyne modified oligonucleotides. 100
Figure 6.3	Anionic exchange chromatogram of crude mixture of 1P ₂₈₀ -1ssD ₉ after click reaction. 103
Figure 6.4	UV absorption at 260 nm for each fraction collected in the gel permeation column separation of 1P ₂₈₀ -1ssD ₉ . 104
Figure 6.5	UV-Vis spectra of PNIPAAm homopolymer and PNIPAAm- <i>block</i> -DNA bioconjugates. 104
Figure 6.6	GPC-MALLS chromatograms of PNIPAAm A. linear and B. three-arm star homopolymers, and PNIPAAm- <i>block</i> -DNA C.linear and D. four-miktoarm star bioconjugates. 109

	Page
Figure 6.7	Transmittance at a wavelength of 500 nm of A. linear and B. three-arm star PNIPAAm homopolymer, and DSC heating scan thermograms of C. linear and D. three-arm star PNIPAAm homopolymers. 111
Figure 6.8	Cloud points (T_{cp}) of linear and three-arm star PNIPAAm homopolymers as a function of degree of polymerization (DP). 112
Figure 6.9	FTIR spectra of PNIPAAm homopolymer and PNIPAAm- <i>block</i> -DNA bioconjugates. 114
Figure 6.10	DSC thermograms of A. linear and B. four-miktoarm star PNIPAAm- <i>block</i> -DNA bioconjugates. 117
Figure 6.11	A. DSC peak temperature (T_p) and B. enthalpy of transition (ΔH) for PNIPAAm homopolymers and their bioconjugates derived from the DSC heating curve. 118
Figure 7.1	Hydrodynamic radii (R_h) of particles formed from linear and four-miktoarm star PNIPAAm- <i>block</i> -DNA bioconjugates A. plotted as a function of $DP_{PNIPAAm}$ for the bioconjugates with 9-mer ssDNA and B. plotted as a function of DP_{DNA} . 125
Figure 7.2	A. Fluorescence emission spectra collected upon heating from 10 to 60 °C, B. emission intensity dependences of temperature at 625 nm and maximum emission wavelength for Nile Red ($\lambda_{exc} = 550$ nm), and repeated heating-cooling cycles of C. fluorescent emission intensity and D. maximum emission wavelength of Nile Red ($\lambda_{exc} = 550$ nm), in the solution of 0.5 mg mL ⁻¹ of 1P ₂₈₀ -1ssD ₉ in 10 mM PB (pH 7.4). 127
Figure 7.3	SAXS profiles obtained at elevated temperatures for sample solution of A. 1P ₃₉₉ -1ssD ₉ and B. 3P ₃₇₀ -1ssD ₉ bioconjugates. 131
Figure 7.4	Guinier plots for A. linear and B. four-miktoarm star PNIPAAm- <i>block</i> -DNA bioconjugates. 132
Figure 7.5	A. Radii of gyration (R_g) and B. particle association number (N_{ass}) dependences of temperature of 1P ₃₉₉ -1ssD ₉ and 3P ₃₇₀ -1ssD ₉ bioconjugates. 133
Figure 7.6	SAXS profiles (open symbols) and their fittings (solid lines) of A. linear and B. four-miktoarm star PNIPAAm- <i>block</i> -DNA colloidal nanoparticles. 136

LIST OF ABBREVIATIONS

1D	One-dimensional
2D	Two-dimensional
3D	Three-dimensional
ABS	Absorbance
ASOs	Antisense oligonucleotides
ATP	Adenosine 5'-triphosphate
ATRP	Atom transfer radical polymerization
CCD	Charge-coupled device
cDNA	Complementary deoxyribonucleic acid
CTP	Cytosine 5'-triphosphate
CuAAC	Copper-catalyzed azide-alkyne cycloaddition
Cys	Cysteine
DLS	Dynamic light scattering
DMAAm	<i>N,N</i> -dimethylacrylamide
DMF	Dimethylformamide
DMSO	Dimethylsulfoxide
DNA	Deoxyribonucleic acid
DNase I	Deoxyribonuclease I
DSC	Differential scanning calorimetry
ds-	Double-stranded-
DTS	DNA-templated synthesis
EPR	Enhanced permeability and retention
FTIR	Fourier transform infrared spectroscopy
GPC	Gel permeation chromatography
GTP	Guanine 5'-triphosphate
HEMA	2-hydroxyethyl methacrylate
HPLC	high performance liquid chromatography
HPMA	<i>N</i> -(2-hydroxypropyl)methacrylamide
LCST	Lower critical solution temperature
MALLS	Multi-angle laser light scattering
MALDI-TOF	Matrix-assisted laser desorption/ionization- time-of-flight mass spectrometer
mRNA	Messenger-ribonucleic acid
MWCO	Molecular weight cut-off
Na-PAA-AAm	Sodium poly(acrylic acid-acrylamide)

NIPAAm	<i>N</i> -isopropylacrylamide
NMR	Nuclear magnetic resonance
NMP	Nitroxide mediated polymerization
PAA	Poly(acrylic acid)
PAGE	Polyacrylamide gel electrophoresis
PB	Phosphate buffer
PBD	Poly(butadiene)
PDEAAm	Poly(<i>N,N</i> -diethylacrylamide)
PDMAAm	Poly(<i>N,N</i> -dimethylacrylamide)
PEG	Poly(ethylene glycol)
PEI	Poly(ethyleneimine)
PEO	Poly(ethylene oxide)
PI	Poly(isoprene)
PLA	Poly(lactide)
PLGA	Poly(D,L–lactic–glycolic acid)
PLL	Poly(L-lysine)
PMA	Poly(methacrylic acid)
PMPC	Poly(methacryloyloxyethylphosphorylcholine)
PMVE	Poly(methyl vinyl ether)
PnBA	Poly(<i>n</i> -butyl acrylate)
PNIPAAm	Poly(<i>N</i> -isopropylacrylamide)
PPO	Poly(propylene oxide)
PS	Poly(styrene)
PUNB	Poly(urethane nitrobenzyl)
RAFT	Reversible addition fragmentation transfer polymerization
RNA	Ribonucleic acid
R-RAFT	Radical reversible addition fragmentation transfer polymerization
RP-HPLC	Reverse-phase high-performance liquid chromatography
SAXS	Small-angle X-ray scattering
SSNa	Sodium styrenesulfonate
ss-	Single-stranded-
TBTA	Tris(benzyltriazolylmethyl)amine
THF	Tetrahydrofluran
Thr	Threonine
UCST	Upper critical solution temperature
UTP	Uracil 5'-triphosphate
UV-Vis	Ultraviolet-visible spectroscopy
Val	Valine

LIST OF SYMBOLS

α -	Alpha-
a.u.	Arbitrary unit
C	Weight concentration
C_p	Specific heat
Cu (I)	Copper I
CuBr	Copper (I) bromide
[CuBr]	Concentration of copper (I) bromide
dn/dc	Differential index of refraction
$(dn/dc)_{DNA}$	Differential index of refraction of DNA
$(dn/dc)_{PNIPAAm}$	Differential index of refraction of PNIPAAm
DP	Degree of polymerization
$DP_{PNIPAAm}$	Degree of polymerization of PNIPAAm
DP_{DNA}	Degree of polymerization of DNA
$^{\circ}$	Degree
$^{\circ}C$	Degree Celsius
ΔH	Enthalpy change of phase transition
g	Gram
GeV	Gigaelectron-volt
h	Hour
[I]	Initiator concentration for ATRP
$I(0)$	zero-angle scattering intensity
$I(q)$	Intensity in the function of momentum transfer
kDa	Kilodalton
λ	Wavelength
λ_{exc}	Excitation emission wavelength
λ_{max}	Maximum emission wavelength
LiBr	Lithium bromide
M	Molar mass
M	Molar
[M]	Concentration of monomers for ATRP
Me₆TREN	tris[2-(dimethylamino)-ethyl]amine
[Me₆TREN]	Concentration of tris[2-(dimethylamino)-ethyl]amine
mg	Milligram
M_n	Number average molecular weight

$M_{n,th}$	Theoretically calculated number average molecular weight
min	Minute
mL	Milliliter
mM	Millimolar
mol	Mole
μL	Microliter
μm	Micrometer
M_w	Weight average molecular weight
n	Number density of particles
N_A	Avogadro's number
NaCl	Sodium chloride
NaN₃	Sodium azide
NaNO₃	Sodium nitrate
[NaNO₃]	Concentration of sodium nitrate
N_{ass}	Particle association number
nm	Nanometer
μ_2/Γ^2	Polydispersity index by cumulant analysis
$P(q)$	Form factor of scattering object
q	Momentum transfer
R_g	Radius of gyration
R_h	Hydrodynamic radius
ρ	Electron density
Psi	Pound per square inch
$P(q)$	Structure factor of scattering object
T	Temperature
T_{cp}	Cloud point temperature
T_p	Endothermic peak temperature
v	Specific volume
W_{DNA}	Weight fraction of DNA
$W_{PNIPAAm}$	Weight fraction of PNIPAAm

Parameters in Core-shell structural model

$A(q)$	Amplitude of scattering object
$D(R)$	Gaussian distribution in the function of particle radius
ξ	Special correlation length in Lorentzian function
$\Delta\rho_{core}$	Contrast of electron densities of core

$\Delta\rho_{\text{shell}}$	Contrast of electron densities of shell
$\Phi(q, R, \sigma)$	Core-shell particle form factor
$I_{\text{fluct}}(q)$	Intensity fluctuation of Lorentzian function
$I_{\text{fluct}}(0)$	Special fluctuation coefficient in Lorentzian function
Γ_{DNA}	Number of DNA per surface area of core particle
L_{shell}	Overall shell thickness
R	Radius
R_{core}	Overall core radius
R_{particle}	Overall particle size
R_{total}	Overall particle radius including the outer interface
$\langle R \rangle$	Mean particle radius
$\rho(r)$	Radial density profile of core-shell particle
ρ_{core}	Density of particle core
S_{DNA}	Surface area occupied by one ssDNA block
σ	Width of interface
σ_{in}	Graded interfaces between core and shell
σ_{out}	Graded interfaces between shell and solvent
σ_{poly}	Gaussian standard deviation
V_{core}	Partial volumes of core
V_{shell}	Partial volumes of shell
W_{core}	Central core width
W_{shell}	Central shell width

Parameters in Baxter Sticky Hard-sphere structural model

$C(q)$	Fourier transform of the direct correlation function
$\delta - D_{\text{hs}}$	Width of square well attraction potential
D_{hs}	Hard sphere diameter
R_{hs}	Hard sphere radius, half of D_{hs}
τ^{-1}	Stickiness parameter in Baxter model
η	Volume fraction of particle
r	Distance between two interacting particles
$U(r)$	Sticky hard sphere potential in $k_{\text{B}}T$ unit
$k_{\text{B}}T$	Boltzmann constant at given temperature
$\alpha, \beta, \mu, \gamma, \varepsilon, \lambda, \chi$	Parameters defined in Equation 5.4

SINTESIS DAN PENCIRIAN BIOKONJUGAT TERMORESPON POLI(*N*-ISOPROPILAKRILAMIDA)–DNA

ABSTRAK

DNA rantai-tunggal (ss) bercabangan dari rantaian polimer utama, poli(*N*-isopropilakrilamida) disintesis melalui pempolimeran radikal untuk menghasilkan biokonjugat PNIPAAm–*graft*–DNA. Segmen PNIPAAm dalam biokonjugat mengalami fasa peralihan apabila suhu meningkat melebihi suatu suhu kritikal (LCST) dan bergabung antara satu sama lain untuk membentuk koloid nanopartikel dalam medium akues. Apabila ssDNA di nanopartikel ini berpasangan dengan DNA komplen untuk menjadi DNA dwi-rantai (ds), nanopartikel ini akan beragregat dalam kemolaran ion garam tertentu dan larutan akan menjadi keruh dengan serta-merta. Fenomena yang dikenali sebagai pengagregatan tidak bertaut-silang tersebut, masih belum difahami sepenuhnya. Selain itu, struktur biokonjugat graft adalah tidak seragam dan mempunyai polidispersiti yang agak tinggi kerana cara sintesis yang sedia ada setakat ini adalah tidak terkawal. Dalam kajian ini, struktur nanopartikel PNIPAAm–*graft*–DNA telah dikajisiasatkan dengan teliti melalui teknik serakan X-ray bersudut-kecil (SAXS). Analisis ini menunjukkan bahawa nanopartikel ini adalah terdiri daripada teras PNIPAAm dan dikelilingi oleh molekul ssDNA sebagai partikel korona. Model struktur dengan “potensi melekit”

telah diaplikasikan kepada analisis SAXS agregat nanopartikel. Analisis ini menunjukkan bahawa nanopartikel beragregat dengan lapisan-lapisan korona sambil bertembusan antara satu sama lain. Tenaga interaksi partikel juga dikuantifikasikan dari segi “potensi melekit”, dan didapati bahawa tren kekuatan interaksi dipengaruhi oleh saiz partikel iaitu, daya van der Waals) dan bukannya kepadatan nombor molekul DNA. Seterusnya, satu laluan sintetik baru iaitu melalui kombinasi pempolimeran radikal transfer atom (ATRP) dan “kimia terklik” untuk mensintesis biokonjugat jenis blok PNIPAAm dan ssDNA (PNIPAAm-*blok*-DNA) dengan komposisi dan arkitektur yang terkawal telah diperkenalkan. Laluan sintetik ini telah ditunjukkan efisien untuk menghasilkan biokonjugat PNIPAAm-*blok*-DNA dengan arkitektur “linear” dwiblok dan blok berbentuk bintang “berlengan empat” dalam pelbagai komposisi. Pada suhu melebihi LCST, blok biokonjugat membentuk nanopartikel yang jauh lebih seragam dan polidispersiti yang lebih rendah berbanding dengan nanopartikel terdiri daripada PNIPAAm-*graft*-DNA yang disintesis melalui laluan pempolimeran radikal konvensional. Struktur nanopartikel PNIPAAm-*blok*-DNA adalah amat bergantung kepada komposisi dan arkitektur rangkaian kopolimer. Pengetahuan yang lebih mendalam dan pemahaman yang lebih jelas tentang fasa peralihan, struktur nanopartikel dan pengagregatan tidak bertaut-silang biokonjugat PNIPAAm-DNA daripada kajian ini dijangka akan

menyediakan platform untuk pengoptimuman aplikasi semasa (iaitu, biosensor dan purifikasi) dan juga inovasi untuk potensi aplikasi masa depan. Tambahan pula, laluan sintetik baru telah diperkenalkan dan ditunjukkan sebagai satu cara yang efisien untuk menghasilkan biokonjugat dengan struktur dan arkitektur terkawal.

SYNTHESIS AND CHARACTERIZATION OF THERMORESPONSIVE POLY(*N*-ISOPROPYLACRYLAMIDE)-DNA BIOCONJUGATES

ABSTRACT

Bioconjugates (PNIPAAm-*graft*-DNA) of poly(*N*-isopropylacrylamide) (PNIPAAm) grafted with single-stranded (ss) DNA were synthesized via radical copolymerization. The bioconjugates self-assembled above its lower critical solution temperature (LCST) in aqueous solution to form micelle-like colloidal nanoparticles. When the ssDNA of the nanoparticle hybridizes with complementary DNA, the particles aggregate above a certain threshold of salt concentration with drastically increased turbidity in solution. The unique properties of the bioconjugates have so far found applications in biosensor and purification. However, the internal structures of the nanoparticles and the non-crosslinking aggregation mechanism have not been fully clarified yet. Moreover, the structures of the graft bioconjugates are less defined due to the uncontrolled synthesis method developed so far. In this study, advanced characterization using mainly small-angle X-ray scattering (SAXS) has provided a detailed structural insight of the PNIPAAm-*graft*-DNA colloidal nanoparticles, leading to a better understanding of the interparticle non-crosslinking aggregation mechanism. The SAXS analyses have provided that the nanoparticle consists of a core

formed by hydrophobic PNIPAAm segments, surrounded by a coronal layer of DNA component in a brush-like structure. A structural model with a sticky potential was applied to the SAXS analysis of the aggregated particles. This analysis provided that the particles aggregated with their coronal layers interpenetrating with each other. The interaction between the particles were quantified in terms of the sticky potential, and showed a trend whereby the attractive interaction is influenced by the nanoparticle size (i.e., van der Waals forces) rather than the graft density of DNA strands on the particle.

The next part of this study reported a new method to prepare well-defined PNIPAAm-*block*-DNA bioconjugates with linear diblock and four-miktoarm architectures via a combination of atom-transfer radical polymerization (ATRP) and “click chemistry”. This method showed good control over the molecular weight and chain architecture for the block bioconjugates. This has led to a better-defined nanoparticles formed (above LCST) as compared to the nanoparticles of PNIPAAm-*graft*-DNA synthesized via conventional method. The better understanding of the nanostructure and aggregation of the PNIPAAm-DNA bioconjugates stem from this study is expected to provide a platform for optimization of the current applications and also innovation for potential future applications.

Furthermore, a novel synthetic route has been introduced and proved to be an effective way to synthesize DNA-encoded bioconjugate with controllable structure and

architecture, thus allowing possibilities of future macromolecular engineering for more sophisticated functional materials.

CHAPTER ONE

Introduction

1.1 General Introduction

The integration of synthetic polymer and biological entities provides an approach to modulate their properties as single entity, forms a new class of hybrid materials, known as bioconjugate (Alemdaroglu and Herrmann, 2007; Borner, 2008). Bioconjugation certainly present tremendous potentials in polymer and material sciences by fully exploiting the diversity of synthetic (polymer) chemistry while expanding its functional complexity with biological systems, prospectively result in materials with superior synergistic properties (Barron and Zuckermann, 1999; Klok, 2005). Peptide/protein-polymer, glycopolymer and DNA-polymer are examples of bioconjugates being extensively researched (Klok, 2005; Alemdaroglu and Herrmann, 2007).

DNA bioconjugates in particular, have received much attention in recent years for several attractive reasons: 1) Single stranded (ss) DNA with any desired sequence, up to hundreds of bases can be easily prepared via solid-phase organic synthesis methods (Caruthers, 1985). In addition, enzymes allow site specific modifications of the DNA strands, thus providing more room to maneuver and to facilitate bioconjugation. 2) From structural point of view, the unique polyanionic

and rigid nature of DNA make it a versatile building blocks for molecular self-assembly (Noro, 2006). 3) Furthermore, because DNA is an informational molecule, the DNA-decorated bioconjugate would also afford its self-recognition property that enables novel biofunctions such as biodiagnostics, targeted drug/gene delivery, separation/purification and detection of DNA.

The development of functional DNA bioconjugates for the specific aforementioned applications would require suitable synthetic polymer counterpart with complementing qualities. “Smart” polymer which is responsive to external stimuli such as pH, light, ionic strength, temperature, etc., provides an element of remote controllability (Schmaljohann, 2006). For instance, poly(*N*-isopropylacrylamide) (PNIPAAm), a well-known temperature-responsive polymer that exhibits a coil-to-globule transition in aqueous solution at its lower critical solution temperature (LCST) (Schild, 1992; Pelton, 2000). The reversible sharp volume phase transition behavior, which causes a sudden change in the solvation state just by a change of temperature, allows PNIPAAm to be tailor-made for specific purpose, and thus make it an excellent candidate for bioconjugation.

Maeda and coworkers have been one of the pioneers of developing PNIPAAm–DNA bioconjugates (Mori et. al., 2001; Mori and Maeda, 2002). Previously, they have prepared PNIPAAm grafted with ssDNA

(PNIPAAm-*graft*-DNA) bioconjugates via radical copolymerization. They have shown that PNIPAAm-*graft*-DNA bioconjugates self-assemble into colloidal particles at temperature above the LCST. The colloidal particles around 50 nm in hydrodynamic diameter disperse stably so that the aqueous solution is still transparent after the micellation. The most remarkable feature is that the colloidal stability strongly depends on the DNA structure (Mori and Maeda, 2002). When the ssDNA hybridizes with its fully complementary DNA, the particles aggregate promptly above a certain threshold of salt concentration. If the double-stranded (ds) DNA contains a single-base mismatch at the free terminus, the DNA-functionalized colloidal particles still remain stably dispersed (Figure 1.1). It is noted that this aggregation of the particles occurs without interparticle molecular linker, known as non-crosslinking aggregation. However, this phenomenon has not been fully clarified yet.

Therefore, PNIPAAm-DNA bioconjugate system is expected as a functional material and has so far found applications in purification of biomacromolecules and biosensing by employing a thermal stimulus (Umeno et al., 1998; Mori et al., 2001; Costioli et al., 2003; Miyamoto et al., 2007). Furthermore, the fully collapsed globular PNIPAAm still contains relatively high water content

(approximately 66%) in its hydrodynamic volume (Wang et al., 1998) which provides for large quantity encapsulation-release of molecules.

Despite the potentials shown by PNIPAAm–DNA bioconjugate system, there has been relatively little progress of researches for more sophisticated applications i.e., DNA-templated synthesis or gene delivery system. One of the reasons for this is the ill-defined structure and broad molecular weight distribution of the as-prepared PNIPAAm–*graft*–DNA bioconjugates due to the low controllability of the conventional radical polymerization method (Schild, 1992) developed so far. Therefore, the resulting particles formed from this type of copolymers are probably also less-defined. Because the copolymer composition and architecture are crucial factors in self-assembly, well-defined copolymers with respect to compositions, architectures and functionalities are essential for the fabrication of DNA-encoded micelles with controllable morphology (Blanazs et al., 2009).

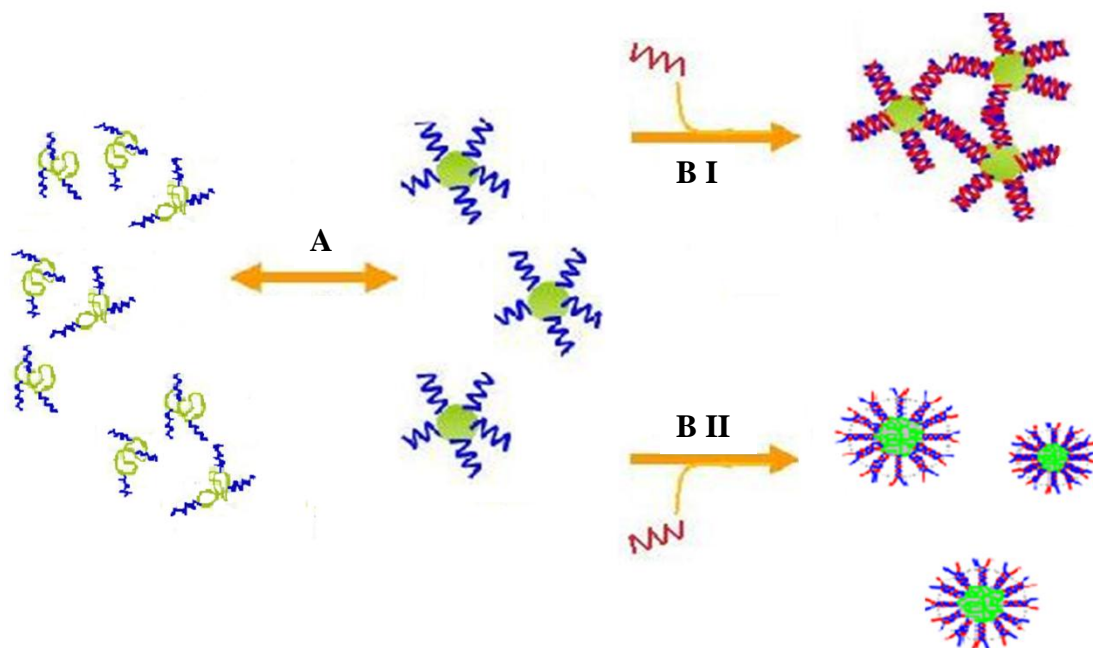


Figure 1.1. Self assembly of PNIPAAm-*graft*-DNA bioconjugates into colloidal nanoparticles and the colloidal stability dependence on its DNA structure.

A. Reversible colloidal particle formation from PNIPAAm-*graft*-DNA bioconjugates at LCST. The colloidal particles consist of dehydrated PNIPAAm core (green) surrounded with hydrophilic ssDNA corona (blue). **B I.** When complementary DNA is added to hybridize with the DNA within the particle, the particles aggregate promptly above a certain salt concentration. **B II.** If target DNA contain a terminal mismatched base pair the particles still remain stably dispersed.

1.2 Hypothesis and Aims of Thesis

This thesis expands upon the previous work of PNIPAAm-*graft*-DNA bioconjugates characterization and focused on micellation of the graft copolymer, its internal structure, dynamism and aggregation at a nanometer scale. Detailed insights of the internal nanostructure is important for understanding of the curious phenomenon of non-crosslinking aggregation, and thus for the optimization of its current applications and also possibly provide a platform for the expansion of future applications such as in microfluidic device and DNA-templated synthesis (DTS).

Furthermore, this thesis attempts to engineer a novel synthesis route to prepare well-defined PNIPAAm block copolymerized with ssDNA (PNIPAAm-*block*-DNA) with controlled compositions and unique architectural designs. The experimental flow is outlined in Figure 1.2.

Specific aims of thesis were:

1. To characterize the nanostructure of colloidal particles formed from PNIPAAm-*graft*-DNA bioconjugates by synchrotron radiation solution small-angle X-ray scattering (SAXS), combined with other techniques.
2. To elucidate the non-crosslinking aggregation mechanism of the PNIPAAm-*graft*-DNA nanoparticles by employing structural models on the SAXS profiles.
3. To improve on the PNIPAAm-DNA bioconjugates synthesis for better control of compositions and architectures via a novel synthetic route.
4. To investigate the composition and architectural effects on the thermo-triggered micellization of the novel PNIPAAm-*block*-DNA bioconjugates and also to evaluate the ability of such micelles to encapsulate and release of hydrophobic guest molecules upon changing temperature.

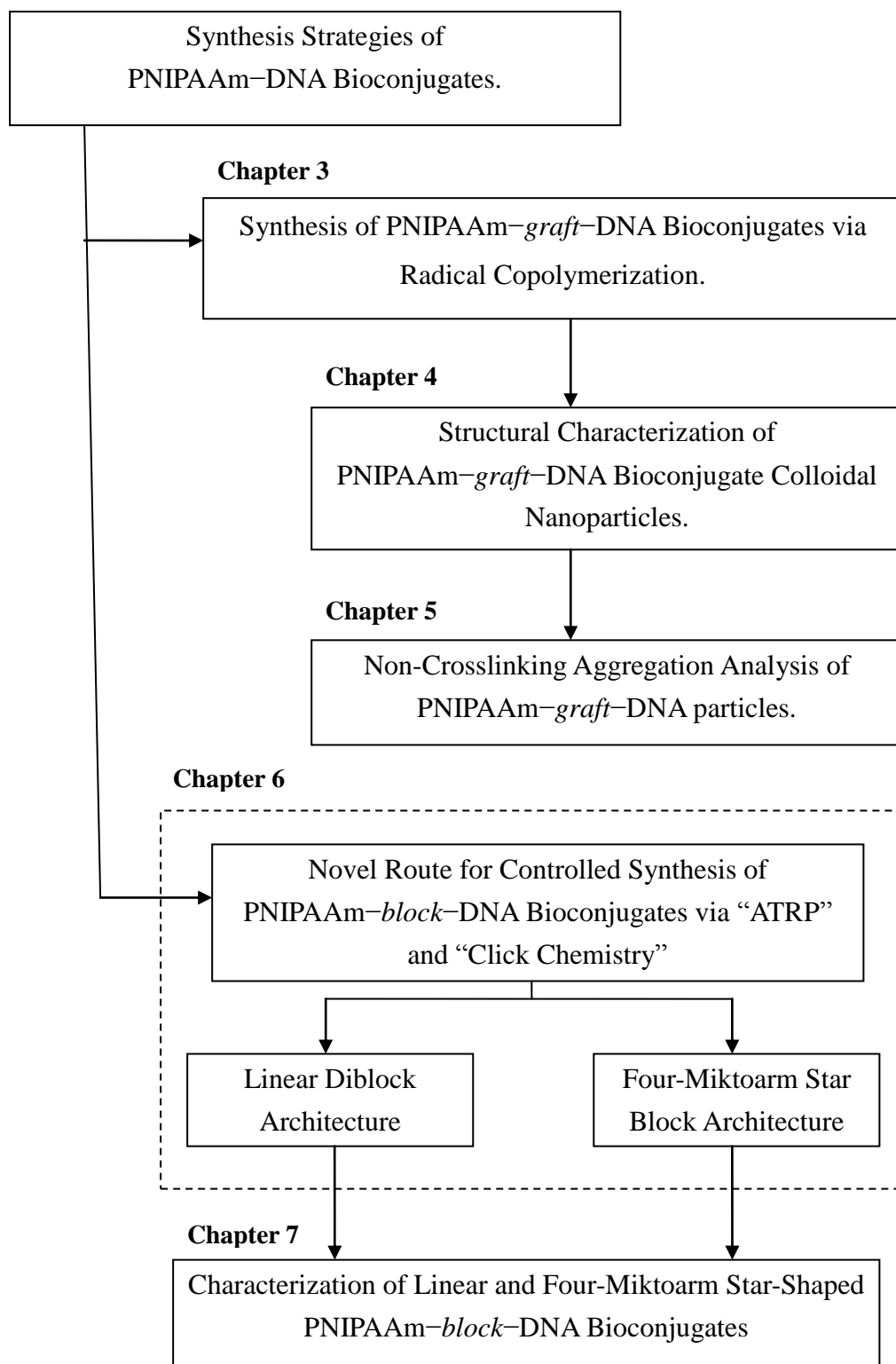


Figure 1.2. Outline and flow of thesis.

CHAPTER TWO

Literature Review

2.1 Bioconjugates

Bioconjugates are hybrid macromolecules of synthetic polymers covalently attached to biological entities such as nucleic acids, peptides, enzymes or cells. Bioconjugates have been initially developed by biochemist solely for biomedical applications (Zalipsky, 1995; Duncan, 2003) have since evolved tremendously in the last decade to become an important field for material science and polymer chemistry (Zhang, 2003; Niemeyer and Mirkin, 2004). For examples, the modern range of application of polymer bioconjugates includes biomedical, bio-sensors, biometrics, photonics and nano-devices (Niemeyer and Mirkin, 2004).

Although biological entities and synthetic polymers share many common features, these two classes of polymers are also characterized by a distinct set of advantages and limitations as outlined in Figure 2.1 (Lehn, 1995). Biological polymers show enormous complexity and specific functionalities but often lack diversity in terms of limited number of building blocks (Börner, 2009). For instances, the construction of complex informational molecules such as DNA is from only four nucleotide building blocks, while, merely 20 α -amino acids are used to generate proteins with exceptional specific functionalities. Even the diverse sequence-defined

oligosaccharides are formed from a rather limited set of building blocks (Werz et al., 2007).

On the other hand, synthetic (polymer) chemistry realizes in-depth diversity from a large set of building blocks. The complexity is however limited in comparison to biological polymers (Börner, 2009). Bioconjugation certainly presents an attractive strategy for polymer and material sciences by combining the advantageous characteristics for both classes of polymers while overcoming their limitations (Cui and Gao, 2003).

There are three main types of polymer bioconjugates: 1) peptide/protein, 2) carbohydrate and 3) nucleotides/DNA bioconjugates. In each type of bioconjugates, the biological systems can be exploited at different levels of their hierarchical organization (i.e., monomeric, oligomeric and polymeric, in the order of increasing complexity/functionality) (Lutz and Börner, 2008). There are also some reports on bioconjugation of highly complex bio-systems such as bacteria or cells which are of the highest degree in terms of functional complexity (Lutz and Börner, 2008). In this chapter, a comprehensive overview of the main types of polymer bioconjugates will be reviewed and particular attention will be paid to nucleotide/DNA bioconjugates and its properties, current applications and synthesis strategies.

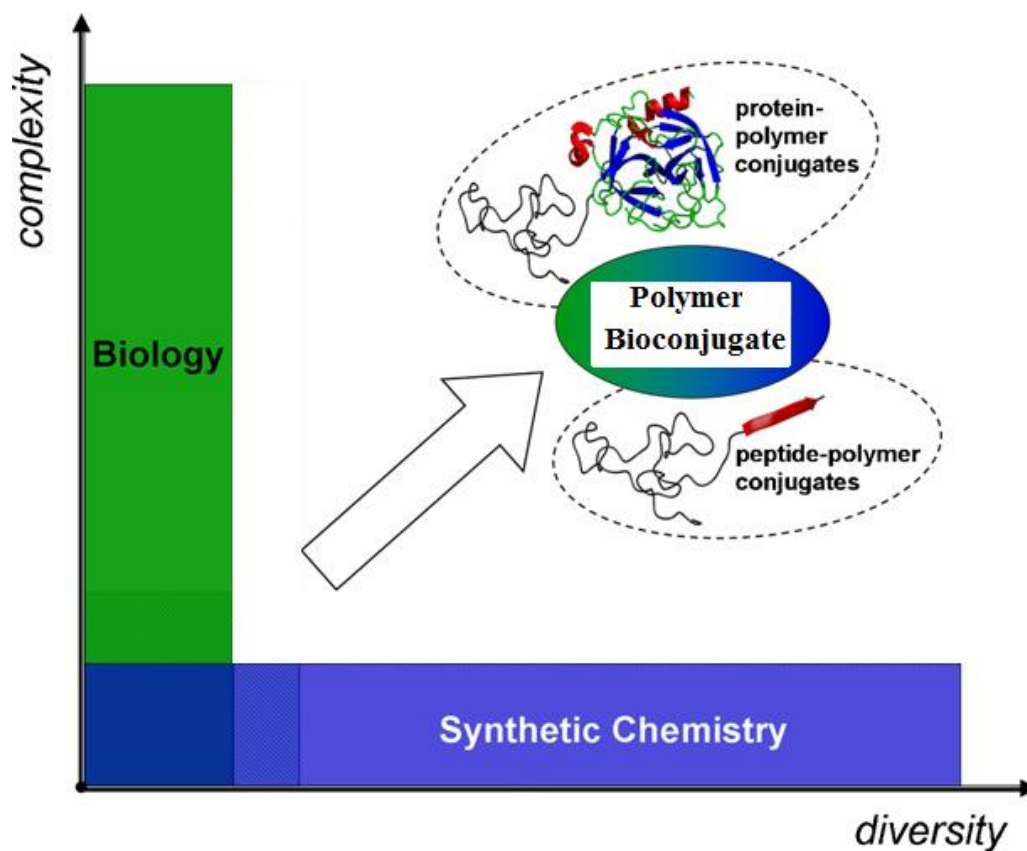


Figure 2.1 A comparison of biological versus synthetic systems with respect to complexity and diversity.

Illustration emphasizes the large void spaces that were filled by neither biological nor synthetic systems and the bioconjugation approaches could potentially fill those void spaces by exploiting the advantages while overcoming the limitations of both polymer classes in terms of complexity and diversity. Figure adapted from Lehn (1995).

2.1.1 Peptide/protein Bioconjugates

Peptide/protein bioconjugates are the most widely studied of all the types of bioconjugates. The broad spectrum of peptide/protein bioconjugates encompasses a range from the simplest structure of polymer-amino acids to highly complex structure of polymer-quaternary protein bioconjugates. With increasing complexity, the chemical diversity of the bio-segments increased dramatically, thus enlarging the functional space. This makes the realization of more complex functions and highly purpose defined properties possible.

The applications of pharmaceutically active peptides, proteins or antibody-based drugs have common limitations which include short plasma half-life, poor stability and triggering of immunogenicity responses (Harris and Chess, 2003; Duncan, 2003). It was discovered that these problems can be significantly reduced by conjugation with poly(ethylene glycol) (PEG) to the peptide of interest (Abuchowski et al., 1977; Davies, 2002). PEG chain is highly flexible, soluble in water and reportedly biocompatible, and therefore the addition of PEG to the peptides (this process also known as PEG-ylation) leads to increased solubility and stability against enzymatic degradation and reducing immunogenicity by acting as a shield around protein, and thus results in increased efficiency and plasma half-life.

Furthermore, it has been reported that the PEG-ylated proteins are able to passively direct anticancer agents specifically to tumor tissue without the need for specific targeting ligands via a mechanism known as enhanced permeability and retention (EPR) effect (Maeda, 2001). The EPR effect is explained in terms of the disorganized pathology of tumor tissue with its discontinuous endothelium and combination of ineffective lymphatic drainage, which accounts for the preferential accumulation of the PEG-modified drugs in tumor cells (Maeda, 2001).

Besides applications in pharmacology, Shi and coworkers (2009) have recently demonstrated an artificial oxygen carrier constructed by conjugating hemoglobin molecules to biodegradable micelles. The micelles are composed of triblock copolymer of PEG, poly(methacryloyloxyethylphosphorylcholine) (PMPC) and poly(lactide) (PLA) (PEG-PMPC-PLA). These polymers are biocompatible and completely biodegradable in the body and thus, do not leave any harmful side effects. In aqueous solution the amphiphilic triblock copolymers forms three-layer micelles with PEG as shell, PMPC as outer core and PLA as inner core as depicted in Figure 2.2. Through the progargyl groups on the PMPC layer, hemoglobin molecules were conjugated to the micelles via click chemistry. The PEG shell acts as shield against immugenicity and enzyme degradation without obstructing the diffusion of oxygen to the hemoglobins.

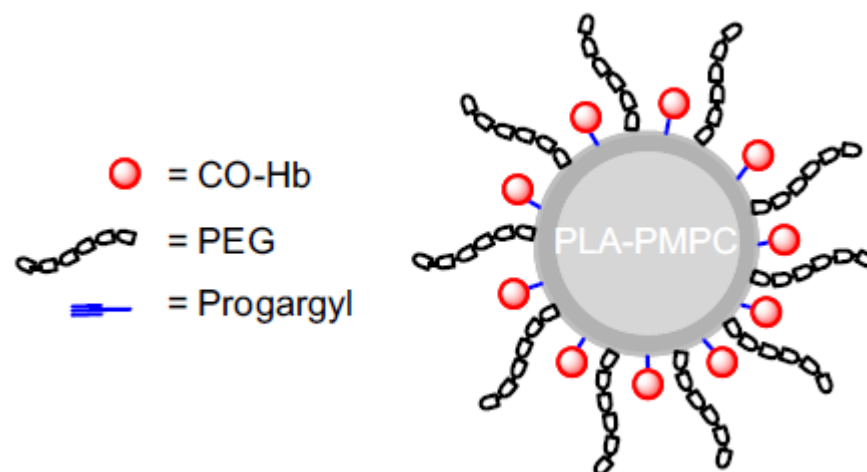


Figure 2.2 Artificial oxygen carrier constructed by conjugating hemoglobin molecules to biodegradable polymeric micelles.

The polymeric micelles are composed of triblock copolymers of PEG-PMPC-PLA which are biocompatible and completely biodegradable in the body. In aqueous solution the amphiphilic triblock copolymers forms three-layer micelles with PEG as shell, PMPC as outer core and PLA as inner core. The PEG shell acts as fluid shield against immunogenicity and degradation by enzymes without obstructing the diffusion of oxygen. The progargyl symbols are partially blocked by the conjugated CO-Hb.

Figure adapted from Shi et al. (2009).

Other examples of peptide/protein bioconjugates and its unique properties are summarized in Table 2.1. Among these examples are peptide bioconjugates that show directed self-assembly and the incorporation of short sequence of amino acids in

synthetic polymers.

Table 2.1 Examples of peptide/protein bioconjugates and its unique properties.

Bioconjugates^a	Properties	References
Cys-containing oligopeptides grafted to PBD- <i>block</i> -PEO	Amphiphiles, self-assembly and superstructures	Geng et al., 2006
(Val-Thr) ₅ -domain-PEO	Organization into well-defined tape-like structures	Hentschel et al., 2006
PDEAAm-streptavidin	Thermoresponsive modulation of activity	Ding et al., 2001
Endoglucanase-DMAAm	Thermoresponsive molecular switch	Shimoboji et al., 2003
HPMA-antibody Fab'	Targeted drug delivery for cancer	Lu et al., 2002

^aAbbreviations: Cysteine (Cys), poly(butadiene) (PBD), poly(ethylene oxide) (PEO), Valine (Val), Threonine (Thr), poly(*N,N*-diethylacrylamide) (PDEAAm), *N,N*-dimethylacrylamide (DMAAm), *N*-(2-hydroxypropyl)methacrylamide (HPMA).

2.1.2 Carbohydrate Bioconjugates

Carbohydrate bioconjugates such as glycopolymers have received much attention due to its cell-cell recognition properties (Kiessling et al., 2000; Geng et al., 2007). Advances in synthetic chemistry have optimized the preparation of well-defined microstructure and multifunctional glycopolymer bioconjugates which are essential for precise recognition properties (Hawker and Wooley, 2005; Voit and Appelhans, 2010). Furthermore, these well-defined carbohydrate-polymer bioconjugates could be important investigating tools for the elucidation of the

carbohydrate-lectin interaction mechanism (Simanek et al., 1998). Lectins are carbohydrate-binding proteins which are naturally present in most cells surfaces and they are important for specific interaction with carbohydrates in recognition processes. Indeed, the factors influencing this mechanism are still not well understood and various potential applications could stem from a better understanding of this process (Bertozi and Kiessling, 2001).

Besides glycopolymers bioconjugates, there are a number of reported researches to develop carbohydrate bioconjugates aimed at biomedical, industrial and pharmaceutical applications, such as surfactants (Klein et al., 1990), detergents (Wulff et al., 1996), drug release (Kopecek et al., 1992; Murata et al., 1996), scaffold for tissue engineering (Suh and Matthew, 2000) and treatment of infectious diseases (Petronio et al., 1997) including HIV (Yoshida et al., 1999).

2.1.3 Nucleotides/DNA Bioconjugates

Nucleic acids are one of nature most important macromolecules that play a crucial biological role in heredity and protein synthesis. DNA molecule has a number of appealing features for use as bioconjugation material which includes the unique structures and powerful molecular recognition properties providing potential biofunctions in bioconjugates as been pointed out in Chapter 1. In addition, the

minuscule size of DNA, with a diameter of about 2 nanometres (nm), its short structural repeat (helical pitch) of about 3.4 nm, and stiffness with a persistence length of around 50 nm, are useful in the field of nanotechnology (Seeman, 2003). Furthermore, DNA can adopt other superstructures, apart from the usual double helix, such as triple helices, quadruplexes and sophisticated artificial 2D and 3D nanostructures (Seeman, 2003; Rothmund, 2006). Therefore, there have been many publications on DNA bioconjugates with unique properties and specific functionality for a wide range of applications in the fields of biology, biotechnology and nanoscience (Alemdaroglu and Herrmann, 2007).

2.1.3.1 DNA Bioconjugates as Gene Delivery Systems

Antisense oligonucleotides (ASOs) are known for their specific interaction with cytoplasmic mRNA, and therefore able to disrupt specific gene transcription. This activity proves to be useful “gene-silencing” tools for highly selective therapeutic strategy for diseases with dysregulated protein expression (Stein and Cheng, 1993). However, cellular uptake of ASOs is poor and susceptible to enzymatic degradation (Opalinska and Gewirtz, 2002). Jeong and coworkers have tried to address these issues by employing micelles of ASO– poly(D,L-lactic–glycolic acid) (PLGA) bioconjugates (Jeong and Park, 2001). They have shown that the micelles were

transported into the cells more efficiently than pristine ASOs. The biodegradable property of the organic PLGA also enables the release of ASOs in a controlled manner.

In another gene delivery system, DNA–poly(ethylene oxide) (DNA–PEO) bioconjugates form micellar electrostatic complex with polycationic moieties such as poly(ethyleneimine) (PEI) or poly(L-lysine) (PLL) (Jeong et al., 2003). Such system is designed to release the DNA in acidic endosomal environment via acid-cleavable linkage between DNA and PEO. Moreover, it was demonstrated that the DNA–PEO within the polyion complex is stable against deoxyribonuclease (DNase I) (Oishi et al., 2005).

2.1.3.2 DNA Bioconjugates in Nanoscience

Nanotechnology is one of the most rapidly developing research areas in recent years. One of the important objectives in this multidisciplinary field is nanoparticles, which often display sizes in the range of 1–100 nm and size-dependent properties different from the bulk materials (Alemdaroglu and Herrmann, 2007). A method commonly utilized to prepare nanoparticles is by molecular self-assembly of materials in suitable solvents into nanodispersed systems (Hamley, 2003; Forster et al., 2004).

The unique structures and properties of DNA make it a versatile building

blocks for molecular self-assembly to form nanoparticles. This class of nanoparticles can be composed of either inorganic or organic materials. The programmable assembly of DNA-encoded inorganic nanoparticles such as gold colloids typically exhibit rigid hard sphere properties (Mirkin et al., 1996; Sato et al., 2003). On the other hand, soft nanoparticles formed by supramolecular self-assembly of amphiphilic DNA block copolymers exhibit intriguing versatility and dynamism owing to the reversible non-covalent intermolecular interactions (i.e. hydrophobic, van der Waals, hydrogen interactions) (Li et al., 2004; Ding et al., 2007; Jakobsen et al., 2008).

Amphiphilic DNA block copolymers when dissolved in aqueous solution generally form nanoparticles containing a hydrophobic polymeric core and a DNA corona. The advantages of such micelle system such as PLGA-DNA have already been highlighted previously in the applications of gene delivery. Another example of amphiphilic DNA block copolymer system with poly(styrene) (PS) have also been synthesized (Li et al., 2004). Various PS-*block*-DNA copolymers with varying DNA length of 5-mer, 10-mer and 15-mer were studied and it was demonstrated that the diameter of the resulting micelles (8–30 nm) are tailorable with different lengths of the DNA segment. These micelles are applied for the selective hybridization with DNA-coated gold nanoparticles.

Recently, a novel template for DNA-templated synthesis (DTS) has been

achieved using nanoparticles of poly(propylene oxide) (PPO) block DNA (PPO-*block*-DNA) (Alemdaroglu et al., 2006). DTS has emerged as a tool for nucleic acid sensing (Mattes and Seitz, 2001), sequence-specific DNA modifications (Magda et al., 1994), small molecule screening (Gartner et al., 2004) and the discovery of new reactions (Kanan et al., 2004). In the nanoparticle system, several DNA-templated organic reactions proceeded in a sequence-specific manner either at the surface of the micelles or at the interface between the DNA and polymer blocks depending on the position of the reactants functionalization at the DNA terminus (Alemdaroglu et al., 2006).

Apart from the usual spherical morphology, amphiphilic block copolymers may self-assemble into a large number of different supramolecular assemblies including rod-like, vesicular and large compound micelles (Shen and Eisenberg, 2000). The micellar morphology is generally determined by a force balance between free energies of core chain stretching, corona chain repulsion, and the core/corona interfacial tension (Halperin et al., 1992). These are readily tunable by altering the copolymer molecular weight, block composition and solvent quality. Control of the nanoparticle morphologies is crucial for their specific applications. There has been a report on DNA-*block*-PPO micelle morphologies are altered by hybridization of the ssDNA corona to form dsDNA (Ding et al., 2007). While hybridization of DNA block

copolymer micelle with complementary short DNA has no significant change on the structures, however, base pairing with longer DNA templates induced a morphology transformation from spherical into rod-like micelles (Figure 2.3). The Watson-Crick motif aligned the hydrophobic polymer segments along the DNA double helix, which resulted in selective dimer formation on the surface. The length of the resulting rod-like micelles could be precisely controlled by adjusting the number of nucleotides in the templates.

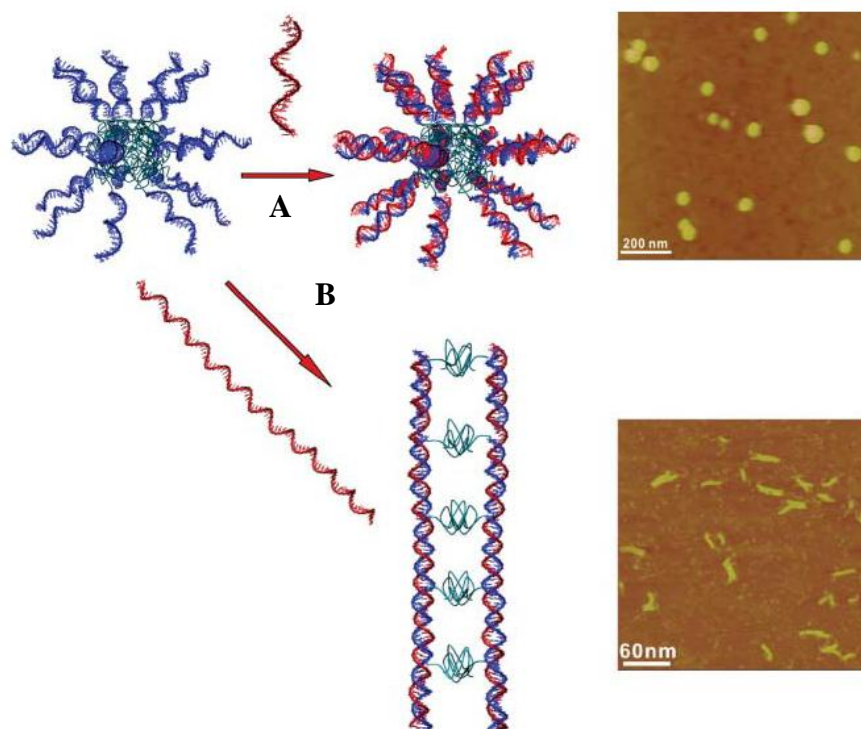


Figure 2.3 Morphologies transformation of ssDNA-*block*-PPO micelles upon hybridization with different length of DNA templates to form dsDNA.

A. Hybridization of DNA block copolymer micelle with complementary short DNA has no significant change on the structures. **B.** Base pairing with longer DNA templates induced a transformation from spherical into rod-like micelles consisting of two parallel aligned double helices. Figures adapted from Ding et al. (2007).

2.1.3.3 DNA–PNIPAAm Bioconjugates

An important emerging class of DNA bioconjugates consists of the DNA–PNIPAAm bioconjugates. As pointed out in Chapter 1, the fully reversible temperature-responsive behavior in PNIPAAm bioconjugation approach has found applications in purification of biomacromolecules and biosensing by employing a thermal stimulus (Umeno et al., 1998; Mori et al., 2001; Costioli et al., 2003; Miyamoto et al., 2007).

The spontaneous selective hybridization property of oligonucleotide with complementary strands has been used for the separation of nucleic acids including mRNA (Tanner, 1989), single- and double-stranded DNA (Imai et al., 1996; Schluep and Cooney, 1998). Traditionally, oligonucleotides-immobilized columns have been used for the isolation of nucleic acids (Bantle et al., 1976). However, the conventional column method has been replaced by a more convenient and smaller scale separation technique using batch-type separation systems (Werner et al., 1984; Hornes and Kornes, 1990). Mori and coworkers (2001) have recently developed a novel batch-type separation system for oligonucleotides using a PNIPAAm–DNA bioconjugates. The bioconjugates has been shown to hybridize with target oligonucleotides to form triple helix structure in a homogenous solution, and the hybrid can be easily separated by heating to above LCST and centrifuging out the

targeted precipitates. It was demonstrated that the separation is highly selective to the targets against equimolar mixtures of oligonucleotides with various one point mutation. In addition, the bioconjugate uses can be recycled repeatedly with constant efficiencies of the 90% targeted oligonucleotides recovered.

Recently, a new application is expanded in the turbidimetric detection of adenosine 5'-triphosphate (ATP) using polymeric micelles of PNIPAAm-DNA bioconjugates (Miyamoto et al., 2007). It is known that, the polymeric micelle with a dehydrated PNIPAAm core surrounded by single-stranded (ss) 11-base DNA (denoted as **DNA1**) corona has drastically lowered colloidal stability when complementary 11-base DNA (**DNA2**) is added to form fully-matched double helix (Mori and Maeda, 2002; Mori and Maeda, 2004). However, when longer complementary 25-base DNA (**DNA3**) is added instead, the colloidal stability remained unchanged (see Figure 2.4). Protrusion of a 14-base ssDNA from the latter hybridization presumably caused entropic repulsion between micelles. Consistently, when 14-base ssDNA (**DNA4**) complementary to the protruding part is added to form singly nicked duplex on the surface, the resulting micelles is remarkably destabilized again as shown in Figure 2.4. Since **DNA3** is an anti-ATP DNA aptamer, which captures two ATP molecules (Huizenga and Szostak, 1995), ATP will competitively inhibit the hybridization of **DNA3** to **DNA1** and alter the colloidal stability of the micelles (Figure 2.5 A). The